

الجمهورية الجزائرية الديمقراطية الشعبية  
PEOPLE'S DEMOCRATIC REPUBLIC OF ALGERIA  
وزارة التعليم العالي والبحث العلمي  
MINISTRY OF HIGHER EDUCATION AND SCIENTIFIC RESEARCH  
جامعة عمّار ثليجي بالأغواط  
AMAR TELIDJI LAGHOUAT UNIVERSITY  
كلية العلوم  
FACULTY OF SCIENCES  
DEPARTMENT Matter Sciences



## ***Master memory***

**Field: Material sciences**

**Faculty : chemistry**

**Option : inorganic chemistry**

**presented by : Behtita Rim**

### **THEME**

---

**Development of new electrode material for the  
electrochemical detection of organic molecules  
of pharmaceutical interest**

---

*Publicly defended before the jury composed of:*

Mr. Saidat Boubakeur	Professor	President
Mr. Sebiane Soufian	Assistant Lecturer	Examiner
Mr. Doulache Merzak	Assistant professor	Reporter

***university year 2019 - 2020***

# *Dedicate*

*I have the great pleasure of dedicating this modest work to:*

*My dear mother.*

*My old brother and his wife (M).*

*My sister and my young brother.*

*And my friends and classmates.*

*for encouragement and give me push up when I  
failed or get tired.*

*I have dedicated to whom think that failed once  
or twice that the end for everything and it is last chance to survive.*

*Never give up on what you want to do.*

*B·Rim*

# Thanks

*Praise and thanksgiving to Allah, the number of atoms of the universe in the heavens and the earth and what is between them and beyond.*

*The best lesson is not learnt from a Book, but from the hearts of truly great teacher.*

*Mr. Doulache M*

*For all hard work and continued efforts that you have made in my education, I will always be thankful, thank you for every advice and information that I have provided or contributed to my access to it. For your working hours and for correcting my mistakes. You will be my role model in the future to be a great professor.*

*All thankful for all professors in Material sciences at Amar Thelidj university, the jury members to have accepted to judge this work.*

*All persons that help me to done this work.*

# Summary

<a href="#">Abstract :</a> .....	1
<a href="#">1. Introduction :</a> .....	3
<a href="#">1.1. Ramipril:</a> .....	3
<a href="#">1.2. Atorvastatin:</a> .....	3
<a href="#">1.3. Combination effect of RAM and ATOR:</a> .....	3
<a href="#">1.4. Simultaneous determination of ATOR and RAM:</a> .....	3
<a href="#">1.5. Electrochemical methods:</a> .....	4
<a href="#">1.6. Chemically modified electrodes:</a> .....	4
<a href="#">1.7. Multi-walled carbon nanotubes (MWCNTs):</a> .....	5
<a href="#">1.8. Aim of this study:</a> .....	6
<a href="#">2. Experimental:</a> .....	6
<a href="#">2.1. Reagents and apparatus:</a> .....	6
<a href="#">2.2. Preparation of the MWCNTs/GCE modified electrode:</a> .....	7
<a href="#">2.3. Analytical procedure:</a> .....	7
<a href="#">2.4. Electroanalytical technique:</a> .....	8
<a href="#">2.4.1. Cyclic voltammetry:</a> .....	8
<a href="#">2.4.2. Pulse Methods:</a> .....	8
<a href="#">2.4.3. Normal pulse voltammetry (NPV):</a> .....	9
<a href="#">2.4.4. Differential Pulse Voltammetry (DPV):</a> .....	9
<a href="#">2.4.5. Square Wave Voltammetry (SWV):</a> .....	10
<a href="#">3. Results and discussion</a> .....	11
<a href="#">3.1. Surface characterization:</a> .....	11
<a href="#">3.2. Electrochemical behavior of ATOR and RAM on MWCNTs/GCE:</a> .....	12
<a href="#">3.3. Effect of MWCNT amounts:</a> .....	14
<a href="#">3.4. Determination of electroactive surface area:</a> .....	15
<a href="#">3.5. The influence of pH:</a> .....	16
<a href="#">3.6. The effect of scan rate:</a> .....	18
<a href="#">3.7. Analytical Parameters:</a> .....	23
<a href="#">4. Conclusion and perspectives:</a> .....	26
<a href="#">REFERENCES:</a> .....	27

## List of figures and scheme

<a href="#">Figure 1 : Geometric structure of MWCNTs</a> .....	6
<a href="#">Figure 2: electrochemical assembly with three electrodes</a> .....	7
<a href="#">Figure 3: (a) Excitation wave form of cyclic voltammetry (b) response obtained for the reversible cyclic voltammetry.</a> .....	8
<a href="#">Figure 4: Excitation waveform of normal pulse voltammetry</a> .....	9
<a href="#">Figure 5: Excitation waveform of differential pulse voltammetry</a> .....	10
<a href="#">Figure 6: a. Excitation waveform of square wave voltammetry. b. Response obtained by square wave voltammetry</a> .....	11
<a href="#">Figure 7: SEM images of the (A) bare GCE and (B) MWCNTs/GCE (C) SEM image with a lower magnification of MWCNTs/GCE.</a> .....	12
<a href="#">Figure 8: Cyclic voltammograms for (A) 0.1 mM ATOR and for (B) 0.1 mM RAM in 0.1 M H<sub>2</sub>SO<sub>4</sub> using a MWCNTs/GCE electrode.(C) CVs of 0.1 mM ATOR and RAM using the bare GCE and MWCNTs/GCE in 0.1 M H<sub>2</sub>SO<sub>4</sub> solution.</a> .....	13
<a href="#">Figure 9: SWV of 0.1 mM ATOR and RAM using the bare GCE and MWCNTs/GCE in 0.1 M H<sub>2</sub>SO<sub>4</sub> solution.</a> .....	14
<a href="#">Figure 10: SW voltammograms obtained with 1×10<sup>-4</sup> M ATOR and RAM in 0.1 M H<sub>2</sub>SO<sub>4</sub> (pH 1.0) using the MWCNTs/GCE sensor with different amounts of MWCNT.</a> .....	15
<a href="#">Figure 11: Cyclic voltammograms for GC electrode and MWCNTs/GC electrode in 5.0 mM K<sub>3</sub> [Fe(CN)]<sup>6+</sup> 0.1 M KCl solution at scan rate of 50 mV s<sup>-1</sup>.</a> .....	16
<a href="#">Figure 12: SWV of 0.1 mM ATOR and RAM on MWCNTs/GCE at different pH values</a> .....	17
<a href="#">Figure13: variation of I<sub>p</sub> as function of pH value (A) ATOR and (B) RAM</a> .....	17
<a href="#">Figure 14: Variation of E<sub>p</sub> as function of pH value (A) RAM and (B) ATOR.</a> .....	17
<a href="#">Figure 15: CVs of MWCNTs/GCE in 0.1 M BRB (pH 3.1) with 0.1 mM ATOR and RAM at different scan rates (5-300 mV s<sup>-1</sup>).</a> .....	18
<a href="#">Figure 14: Logarithmic dependence of I<sub>p</sub> on the logarithmic scan rate values (A) ATOR and (B) RAM.</a> .....	19
<a href="#">Figure 15: the plots of peak current (I<sub>p</sub>) versus potential scan rate (v) (A) ATOR and (B) RAM.</a> .....	19
<a href="#">Figure 16: the plots of peak current (I<sub>p</sub>) versus square root of the scan rate (v<sup>1/2</sup>) (A) ATOR and (B) RAM.</a> .....	20
<a href="#">Figure 19: the plots of peak potential (E<sub>p</sub>) versus logarithmic scan rate values.</a> .....	20
<a href="#">Scheme 1: Proposed electro-oxidation mechanisms of ATOR (a) and RAM (b).</a> .....	22
<a href="#">Figure 20: SWV responses for simultaneous addition of ATOR and RAM from 10 to 100 μM. Experimental conditions: 0.1 M BRB (pH = 3.0) at MWCNTs/GCE.</a> .....	23
<a href="#">Figure 21: The calibration curves for peak current vs. concentration for (A) ATOR and (B) RAM.</a> .....	24

## List of tables

<a href="#"><u>Table 1: Regression data of the calibration curve for quantitative determination of ATOR and RAM by SWV method in bulk solution.</u></a> .....	24
<a href="#"><u>Table 2. Comparison of the analytical parameters obtained using different techniques for the determination of ATOR and RAM.</u></a> .....	25

## **list of abbreviations and symbols**

A: is the electroactive surface area.

ACEI: angiotensin-converting enzyme inhibitor.

ATOR: Atorvastatin.

C: the concentration of the reaction species in the electrolyte

C: the concentration of the reaction species in the electrolyte.

CME: chemically modified electrode.

CV: Cyclic voltammetry.

D : the diffusion coefficient.

F : Faradays constant.

GCE: Glassy Carbon electrode.

HPLC: High performance liquid chromatography.

I<sub>p</sub>: the peak current.

LC/MS/MS: liquid chromatography-tandem mass spectrometry.

LOD: High performance liquid chromatography.

LOQ : quantitation limits.

MWCNTs: Multi-walled carbon nanotubes.

n: the number of electrons transferred in the redox reaction.

Q<sub>eq</sub>: the specific charge equivalent.

RAM: Ramipril.

Redox : Reduction/oxidation reaction.

RP-HPLC: Reversed phase High performance liquid chromatography.

SCE: saturated calomel electrode.

SEM: scanning electron microscope.

SWV: square wave voltammetry.

$\nu$ : is the scan rate.

$\delta$  : the thickness of the Nernst diffusion layer corresponding to the peak current.

## خلاصة:

في هذه المذكرة، تم دراسة السلوك الكهروكيميائي لدواء الأتورفاستاتين (لعلاج ارتفاع الكوليسترول، ATOR) ودواء الرامبيرييل (لعلاج ارتفاع ضغط الدم، RAM) على قطب الكربون الزجاجي المعدل بالأنايبب النانوية الكربونية متعددة الجدران (MWCNTs/GCE). خلال هذه الدراسة تم تطوير تقنية كهروكيميائية بسيطة وحساسة للغاية من أجل التحليل الكمي المتزامن لأتورفاستاتين ورامبيرييل باستعمال طريقة قياس جهد-تيار ذو الإشارة المربعة (SWV) في محلول موقفي BRB (0.1مول/ل و pH=3.0). اظهرت الدراسة ان عملية الاكسدة تتحكم فيها ظاهرة إمتزاز المركبين على سطح القطب المعدل. باستخدام البيانات المتحصل عليها ومناقشتها تم اقتراح آلية أكسدة المركبين التي تحدث على سطح القطب المعدل. التحليل الكهروكيمي باستخدام القطب المعدل أثبت نجاعة تحليلية عالية من ناحية الحساسية لهذين الدوائين ، حيث أظهرت الطريقة المقترحة استجابات خطية في مجال للتراكيز تتراوح بين 10-100 ميكرومول/ل لـ ATOR و RAM مع كشف حدي (LOD) يساوي 2.57 و 1.87 ميكرومول/ل، على التوالي.

**الكلمات المفتاحية:** ، التحليل الكهروكيمي المتزامن للأتورفاستاتين والرامبيرييل ، القطب الكهربائي المعدل، الأنايبب النانوية الكربونية متعددة الجدران ، قياس الجهد الدوري (CV)، تقنية قياس جهد-تيار ذو الإشارة المربعة.

### Abstract:

In this study, the electrochemical behavior of Atorvastatin (ATOR) and Ramipril (RAM) was investigated on multi-walled carbon nanotubes (MWCNTs) modified glassy carbon electrode (GCE) as simultaneously. A simple and highly sensitive square wave voltammetry (SWV) technique was developed for the simultaneous electrochemical determination of ATOR and RAM in 0.1M BRB solution (pH 3.0). The oxidation process of both analytes was found to be irreversible and exhibited mixed diffusion under adsorption-controlled process. The oxidation mechanism of drugs was proposed using the obtained data and discussed. The MWCNTs/GCE showed an enhancement effects on the oxidation current of ATOR and RAM with the significant peak potential differences of 0.27 V by SWV technique. At the optimum conditions, the proposed method exhibited linear responses in concentration ranges 10-100  $\mu\text{M}$  for ATOR and RAM with the detection limits of 2.57 and 1.87  $\mu\text{M}$  respectively.

**Keywords:** Modified electrode, Atorvastatin and Ramipril drugs; MWCNTs; Simultaneous electrochemical assay.

**Résumé :**

Dans cette étude, le comportement électrochimique de l'atorvastatine (ATOR) et du Ramipril (RAM) a été étudié simultanément sur l'électrode de carbone vitreux (GCE) modifiée par les nanotubes de carbone multiparois (MWCNT). Une simple et très sensible technique a été développée pour la détermination simultanée d'ATOR et de RAM dans une solution BRB 0.1M (pH 3.0) en utilisant la voltammétrie à vague carrée (SWV). Le processus d'oxydation de l'ATOR et RAM sur l'électrode modifiée est principalement contrôlés par l'adsorption. Le mécanisme d'oxydation des deux médicaments a été proposé en utilisant les données obtenues et discuté. Par ailleurs, Les deux pics anodiques de l'ATOR et RAM sont séparés par une valeur de  $\sim 0.27$  V, rendant le dosage simultané des deux espèces plus sélective. Dans les conditions optimales, la méthode proposée présente une partie linéaire comprise entre (10-100  $\mu$ M) pour les deux médicaments avec des limites de détection de 2.57  $\mu$ M pour ATOR et 1.87  $\mu$ M pour RAM

**Mots clés :** électrode modifiée, Atorvastatine et Ramipril, nanotubes de carbone multiparois, détection électrochimique

## **1. Introduction :**

### **1.1. Ramipril:**

Ramipril (RAM) is an angiotensin-converting enzyme inhibitor (ACEI), which is widely used to lowering high blood pressure (hypertension), congestive cardiac failure and kidney problem [1], RAM is prodrug converted in the liver by de-esterification into its active form ramiprilat, which inhibits ACE, thereby blocking the conversion of angiotensin I to angiotensin II [2]. However, an overdose of RAM may cause hypotension, bradycardia and other side effects [3]

### **1.2. Atorvastatin:**

Atorvastatin (ATOR) is chemically (3*R*,5*R*)-7-[2-(4-Fluorophenyl)-3-phenyl-4(phenyl carbamoyl)-5-propan-2-ylpyrrol-1-yl]-3,5-dihydroxyheptanoic acid. Atorvastatin is an antilipidemic agent and it is a member of the drug class known as statins. It is an inhibitor of 3-hydroxy-3-methylglutaryl-coenzyme A (HMG-CoA) reductase enzyme that participates in the endogenous cholesterol synthetically (3*R*,5*R*)-7-[2-(4-Fluorophenyl)-3-phenyl-4-(phenylcarbamoyl)-5-propan-2-ylpyrrol-1-yl]-3,5-dihydroxyheptanoic acid. The drug is odourless white crystalline powder and practically insoluble in water, soluble in ethanol, Atorvastatin is more potent and appears to have the highest LDL-CH lowering efficacy. [4]

### **1.3. Combination effect of RAM and ATOR:**

Atorvastatin and Ramipril are available in the market as a single or as combination dosage form an antihypertensive agent found to be therapeutically very effective in cardiac patients, This combination is widely started to use in India in the trade name Stator-R 5 [5].

Analytical Chemistry is the branch of science that uses advance technologies in determining the composition by analytical technique. We can achieve both qualitative as well as quantitative results.

### **1.4. Simultaneous determination of ATOR and RAM:**

In the literature, few methods were reported for the determination of these drugs either individually or in combination in pharmaceutical dosage forms. These methods include spectrophotometric methods [6], HPLC methods [7], LC/MS/MS methods [8] were reported. Only stability-indicating methods with the combination of these drugs is available, and no official method for the simultaneous estimation of ATOR and RAM is available, the author developed and validated a cost-effective RP-HPLC assay method for the drugs, in fixed dosage formulation as per ICH and other relevant guidelines [9]. Based on the intended purpose and scope of the analytical method, the important parameters that may be evaluated

during method development are specificity, linearity, limits of detection (LOD) and quantitation limits (LOQ), range, accuracy and precision [10].

Nevertheless, most of these methods are time-consuming, expensive instrumentations and involve tedious sample preparations or, on the other hand, suffer from poor selectivity. Consequently, a cheap, highly sensitive and selective method is of great demand for simultaneous determination of ATOR and RAM.

### **1.5. Electrochemical methods:**

On analytical techniques that use a measurement of potential, charge, or current to determine an analyte's concentration or to characterize an analyte's chemical reactivity. Collectively we call this area of analytical chemistry electrochemistry because it originated from the study of the movement of electrons in an oxidation–reduction reaction[11] Ascertain molecules are oxidized or reduced (redox reactions) at the working electrode (e.g. Pt, Au, carbon, etc.) [12], The application of electrochemical methods to systems containing low concentrations of supporting electrolyte is challenging. [13] Electrochemical methods traditionally have found important applications in sample analysis, and organic and inorganic synthesis. The electrode surface itself can be a powerful tool. By controlling the potential, the electrode can be used as a variable free energy source (or sink) of electrons. Also, electrons crossing the electrode-solution interface can be determined with great sensitivity by measuring current. [14] The analytical advantage of various electrochemical techniques include excellent sensitivity with very large useful linear concentration, a large number of useful solvents and electrolytes, rapid analysis times, simultaneous determination of analytes, the ability to determine kinetics and mechanistic parameters, a well-developed theory and thus the ability to reasonably estimate the values of unknown parameters, and the ease with which different potential waveforms can be generated and small current measured.

### **1.6. Chemically modified electrodes:**

The IUPAC [15], defined a chemically modified electrode (CME) as an electrode made of a conducting or semiconducting material that is coated with a selected monomolecular, multimolecular, ionic, or polymeric film of a chemical modifier and that by means of faradic (charge transfer) reaction or interfacial potential differences (no net charge transfer) exhibits chemical, electrochemical, and/or optical properties of the film. These modifications involve irreversible adsorption [16], self-assembled layers [17] , covalent bonding [18], electro polymerization [19] , and others. Surface modifications play a catalytic role and very small

changes in surface characteristics determine the sensitivity of measurement in electroanalytical applications. Factors affecting the response of a modified electrochemical sensor include the nature of coating material, method of synthesis of coating material, mechanism of electrode coating, use of mediators, and nature of sample matrix [20].

Modification of the conductive substrate may result in enhanced electron transfer kinetics. Glassy carbon is among the most commonly used substrates for modification as it provides a wide potential window with low background currents and it is chemically stable. The use of chemically modified electrodes can help in selective, sensitive, and reproducible detection of ATOR and RAM in the presence of other interferences by reduction of ohmic resistance associated with the wide potential window [21].

### **1.7. Multi-walled carbon nanotubes (MWCNTs):**

Among recent years, carbon nanostructures are in the spotlight of various research fields especially in electroanalytical investigations due to special properties. Multi-walled carbon nanotubes (MWCNTs) are one of the most commonly used carbon nanostructures that have received a remarkable attention in a wide range of applications (Fig.1), especially in electrochemical sensors. The broad application area for MWCNTs is due to their fabulous physical and chemical properties, including an extremely large surface area to volume ratio, appropriate conductivity, high porosity and loading, nontoxicity, hollow structure, small diameter, special optical and electrical properties and exceptionally high tensile strength. Several authors have reported the excellent electrocatalytic properties of nanotubes in the redox behavior of different molecules and bio-molecules. There are reports on the advantages of CNTs modified electrodes on the electrocatalytic response of hydrazine [22], glucose [23], dihydronicotinamide adenine dinucleotide (NADH) [24], dopamine [25], ascorbic acid [26], hydrogen peroxide [27]. Thus CNTs-modified electrodes have shown interesting catalytic properties toward electrochemical processes. It must be noted that electrodes modified with carbon nanotubes have increased surface areas and adsorption efficiency compared to other common electrodes, and exhibit intriguing ability to enhance the electrochemical responses of several organic molecules [28], thus making them more favorable as electrode materials for the type of investigation reported in this work compared to other common electrodes.

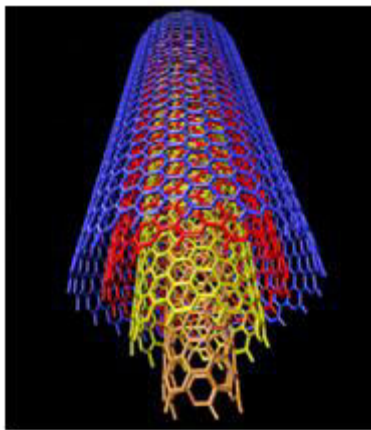


**Figure 1** : Geometric structure of MWCNTs

### **1.8. Aim of this study:**

Up to our knowledge, an electrochemical determination of these two drugs has not been previously described in the literature. Thus, the present work provides a novel method for simultaneous trace analysis of ATOR and RAM at MWCNTs/GCE electrode, which has a significant attraction in biological and chemical fields.

## **2. Experimental:**

### **2.1. Reagents and apparatus:**

ATOR and RAM were obtained from Kocak Pharm. Company (Istanbul, Turkey), 1.0 mM standard stock solutions of ATOR were prepared in ethanol pure and RAM were prepared in distilled water and they put in refrigerator to keep fresh.  $\text{H}_2\text{SO}_4$  (0.1M) and 0.04 M Britton-Robinson buffer (prepared by mixing 0.04 M  $\text{H}_3\text{PO}_4$ ,  $\text{CH}_3\text{COOH}$  and  $\text{H}_3\text{BO}_4$ ) solutions were used for the preparation of buffer solutions at pH range 0.3-7.0. The pH values were adjusted to the related pH by 5 M sodium hydroxide (Fluka) under the pH-meter. The other chemicals were analytical grade. All solutions were prepared in distilled water.

All electrochemical measurements were realized using a three-electrode cell at ambient temperature; the data was recorded with a potentiostat/galvanostat PGZ402 coupled with a PC-computer (Fig. 2). A three-electrode system was used for all measurements;  $\text{Hg}/\text{Hg}_2\text{Cl}_2$  (saturated KCl) as the reference electrode, Pt wire as the counter electrode and GCE ( $\text{Ø} = 3$  mm) and MWCNTs/GCE as the working electrodes. The pH was controlled with a pH meter INOLab pH7110 instrument.



**Figure 2:** *electrochemical assembly with three electrodes*

For the analytical application, Potential cyclic voltammetry; potential from -250 to 1700 mV at scan rate 50mV/s. The optimum SWV parameters were given a follow; potential 0 to 1700 mV; amplitude potential 10 mV; scan rate 10 mV/s; pulse potential 50 mV at duration 1s.

### **2.2.Preparation of the MWCNTs/GCE modified electrode:**

Initially, the GCE was polished to mirror-like surface with alumina (0.05-0.3 mm) slurry on a polishing cloth. After being rinsed with distilled water, the polished GCE was sonicated for 5 min in ethanol and dried at room temperature.

The MWCNTs suspension was prepared by dispersing 10 mg of functionalized MWCNTs into 10 mL of N,N-dimethylformamide (DMF) solvent under ultrasonic agitation for 30 min. The MWCNTs/GCE was made by dropping volumes of MWCNTs suspension on the electrode surface using a micropipette and leaving it to dry at 90°C 10 min in heating and drying ovens. Due to the evaporating solvent, a uniform and stable MWCNTs film was obtained on the electrode surface.

### **2.3.Analytical procedure:**

The MWCNTs/GCE was first stabilized in 0.1 mol L<sup>-1</sup> BRB solution (pH 2.0) by 3 cyclic voltammetric sweeps in potential range of 0 V to 1.7 V. Then, the used sensor was transferred into a 10 mL glass conventional cell containing 0.1 M BR buffer solution (pH 3.0), and aliquots of the stock solution of drugs were added.

The analytical curve was constructed using the SW voltammograms obtained after the successive addition of aliquots of the drugs (RAM and ATOR) stock solution into the electrochemical cell containing 10 mL of 0.1 M BRB solution (pH 3.0). Each concentration was a measurement in triplicate.

## 2.4. Electroanalytical technique:

### 2.4.1. Cyclic voltammetry:

Cyclic voltammetry consists of cycling the potential of an electrode, which is immersed in unstirred solution and measuring the resulting current. The potential of the working electrode is controlled versus a reference electrode. The controlling potential that is applied across these two electrodes can be considered an excitation signal. The excitation signal for cyclic voltammetry is linear potential scan with a triangular wave form as shown in Fig. 3. This triangular potential excitation signal sweeps the potential of the electrode between two potentials sometimes called the switching potential [29]

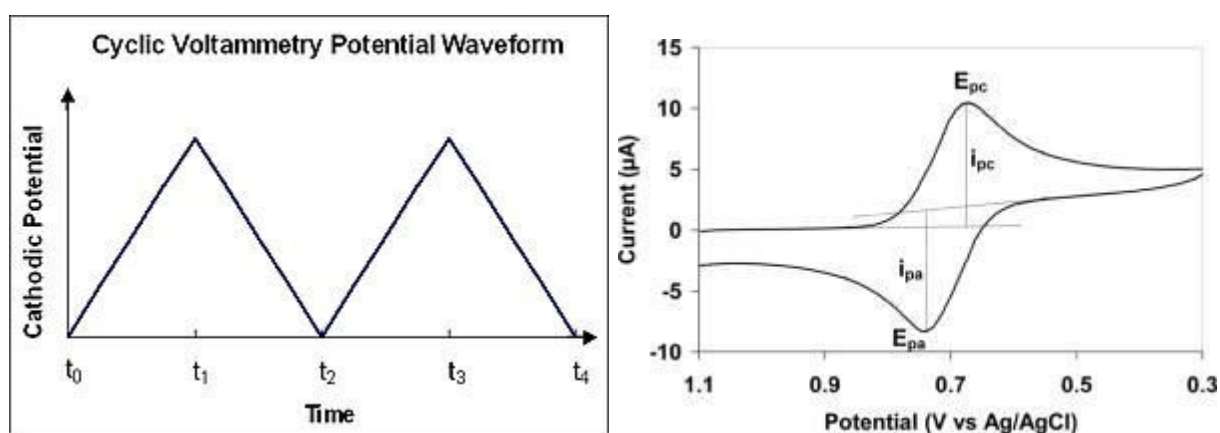


**Figure 3:** (a) Excitation wave form of cyclic voltammetry (b) response obtained for the reversible cyclic voltammetry.

A cyclic voltammogram is obtained by measuring the current at the working electrode during the potential scan. The current measured can be considered as the response signal to the potential excitation signal. The voltammogram is a display of current (vertical axis) versus potential (horizontal axis). Because the potential varies linearly with time, the horizontal axis can also be thought as time axis.

The important parameter of a cyclic voltammogram are the magnitude of the anodic peak current ( $I_{pa}$ ), cathodic peak current ( $I_{pc}$ ), anodic peak potential ( $E_{pa}$ ) and cathodic peak potential ( $E_{pc}$ ). A redox couple in which both species rapidly exchange electrons with the working electrode is termed as electrochemically reversible couple.

### 2.4.2. Pulse Methods:

The imposition of potential pulse to the electrode leads to in most experimental situations to a considerable improvement (increase) in the ratio of the charging and faradic currents compared to linear scan voltammetry. This is because the faradic current usually decreases with  $1/t^{1/2}$  while the charging current decreases much faster. In consequence, decreased lower limits of detection are obtained [30].

### 2.4.3. Normal pulse voltammetry (NPV):

This technique uses a series of potential pulses of increasing amplitude (Fig. 4). The current measurement is made near the end of each pulse, which allows time for the charging current to decay. It is usually carried out in an unstirred solution at either DME (called normal pulse voltammetry) or solid electrodes. The potential is pulsed from an initial potential  $E_i$ . The duration of the pulse is usually 1 to 100 ms and the interval between pulses is typically 0.1 to 5 sec. The resulting voltammogram displays the sampled current on the vertical axis and the potential to which the pulse is stepped on the horizontal axis [31].

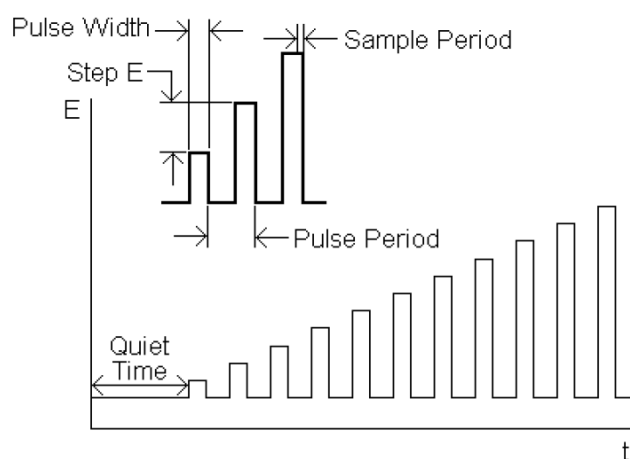


*Figure 4: Excitation waveform of normal pulse voltammetry.*

### 2.4.4. Differential Pulse Voltammetry (DPV):

Differential pulse voltammetry can be considered as a series of regular voltage pulses superimposed on a linearly changing voltage, in which the resulting current is measured between the ramped baseline voltage and the pulse voltage. A digital staircase voltage is commonly used as the ramped baseline (Fig. 5). This technique is comparable to normal pulse voltammetry in that the potential is also scanned with a series of pulses. However, it differs from NPV because each potential pulse is fixed, of small amplitude (10 to 100 mV), and is superimposed on a slowly changing base potential. Current is measured at two points for each

pulse, the first point (1) just before the application of the pulse and the second (2) at the end of the pulse. These sampling points are selected to allow for the decay of the non-faradic (charging) current. The difference between current measurements at these points for each pulse is determined and plotted against the base potential [29][30].

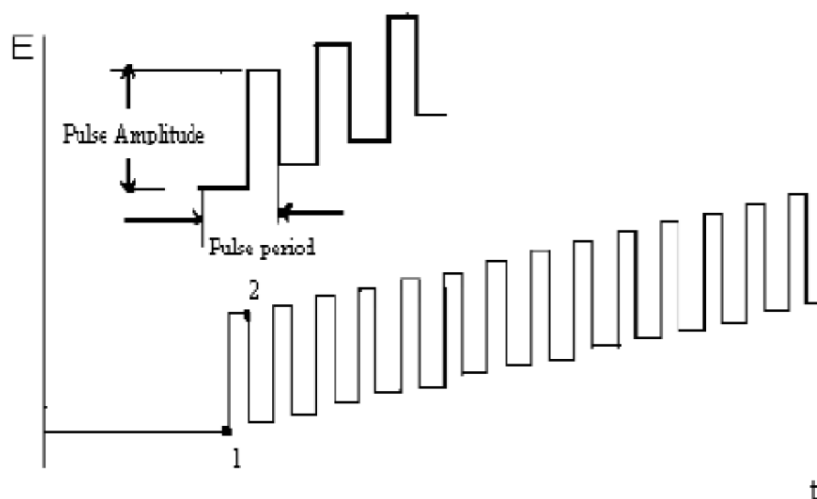


**Figure 5:** Excitation waveform of differential pulse voltammetry

#### 2.4.5. Square Wave Voltammetry (SWV):

Square wave voltammetry is a type of pulse voltammetry that offers the advantage of speed and high sensitivity. An entire voltammogram is obtained in a few seconds or less. The excitation signal in SWV consists of a symmetrical square-wave pulse of amplitude  $E_{sw}$  superimposed on a staircase waveform of step height  $\Delta E_s$ , where the forward pulse of the square wave coincides with the staircase step (Fig. 6). The net current,  $i_{net}$ , is obtained by taking the difference between the forward and reverse currents ( $i_2 - i_1$ ) and is centered on the redox potential. The peak height is directly proportional to the concentration of the electroactive species. Excellent sensitivity is achieved from the fact that the net current is larger than either the forward or the reverse components, since it is the difference between them and detection limits as low as  $1 \times 10^{-8}$  M are possible [31].

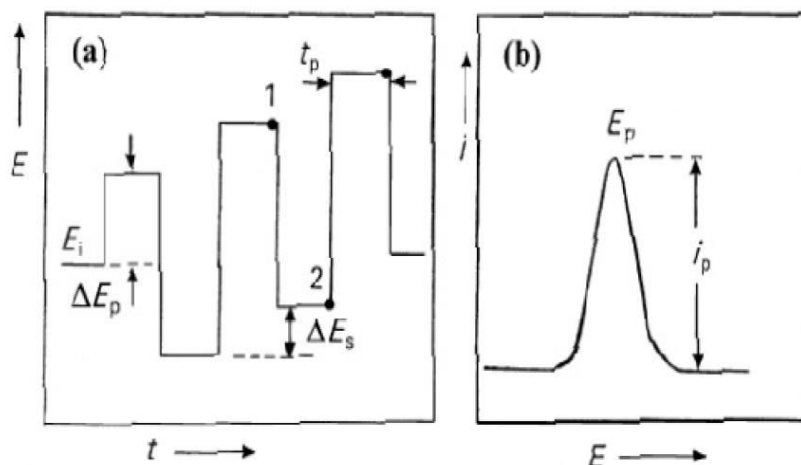


**Figure 6:** a. Excitation waveform of square wave voltammetry. b. Response obtained by square wave voltammetry.

Applications of square-wave voltammetry include the study of electrode kinetics with regard to preceding, following, or catalytic homogeneous chemical reactions, determination of some species at trace levels, and its use in electrochemical detection in HPLC [30].

### 3. Results and discussion

#### 3.1. Surface characterization:

The surface morphology of MWCNTs was characterized using scanning electron microscope (SEM). The homogeneity of MWCNTs is crucial for the purpose of electroanalytical applications. The SEM images of the bare and MWCNTs/GC electrodes are shown in Fig.7A and 7B, respectively. The surface roughness of the MWCNTs/GCE is larger than that of the bare electrode. As shown in Fig.7B, the MWCNTs film offer the huge electroactive surface area and enhance the electron transfer rate on the electrode surface. This means that the MWCNTs will act as a high conductivity wire throughout the MWCNTs and be electrical contact with underlying GCE. This configuration of MWCNTs with a high dispersion of MWCNTs may result in good electro catalytic ability for electrochemical oxidation of ATOR and RAM.

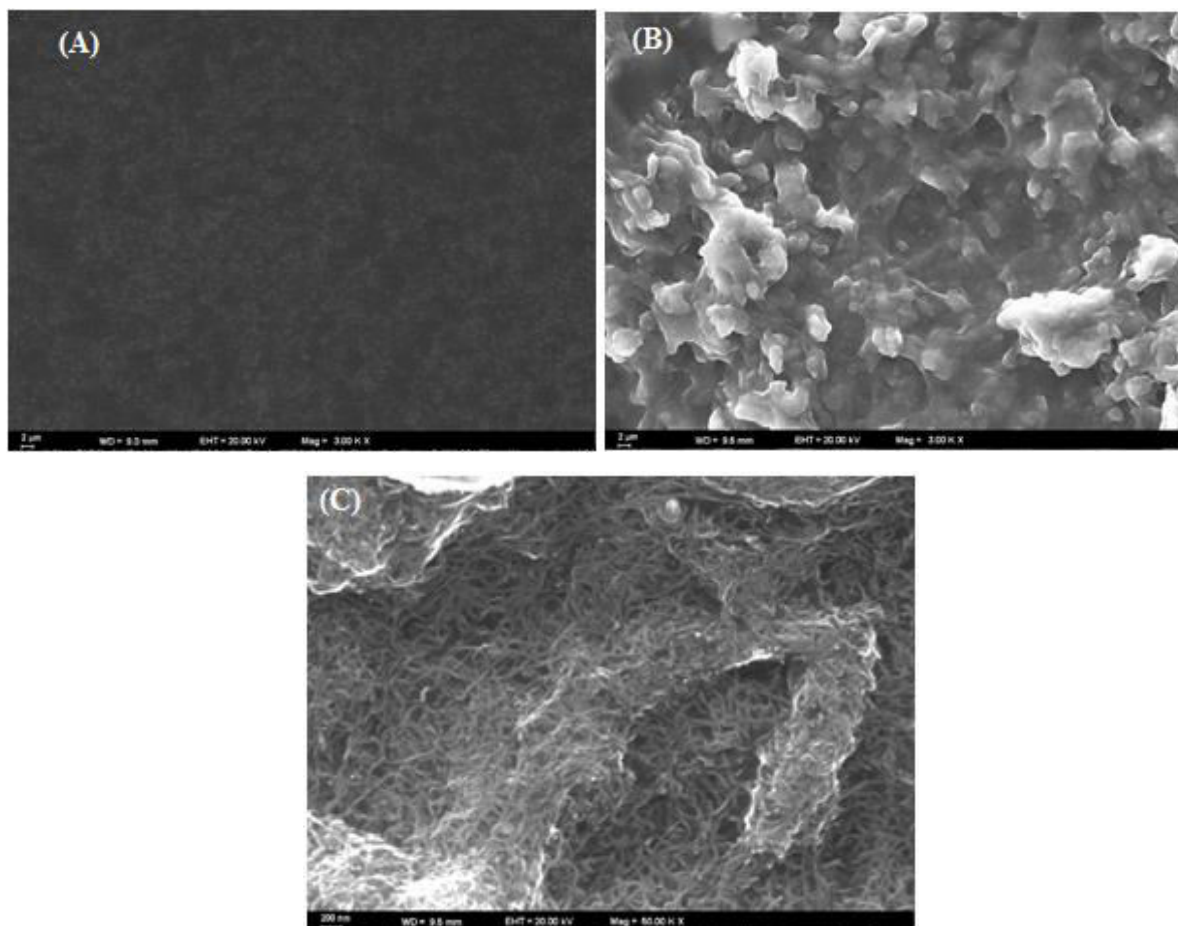


**Figure 7:** SEM images of the (A) bare GCE and (B) MWCNTs/GCE (C) SEM image with a lower magnification of MWCNTs/GCE.

### 3.2. Electrochemical behavior of ATOR and RAM on MWCNTs/GCE:

Fig. 8A, B shows the cyclic voltammograms of 0.1 mM ATOR and RAM at the MWCNTs/GCE electrode. As can be seen, anodic peaks appear at 1.05 and 1.35 V for ATOR and RAM, respectively. For both drugs, no cathodic peaks were observed on the reverse scan within the investigated potential range, indicating totally irreversible electron-transfer kinetics.

The voltammetric behavior of binary mixture ATOR and RAM (0.1 mM) in 0.1 M H<sub>2</sub>SO<sub>4</sub> solution (pH 1.0) on GCE and MWCNTs/GCE electrodes was illustrated in Fig. 8C. At the bare GCE, the ATOR and RAM gave two small anodic peaks at 1.07 V and 1.44 V, respectively and the cyclic voltammogram showed weak and insignificant current responses. Compared with a bare electrode, two well-defined peaks negatively shifted with peak current increase significantly at MWCNTs/GCE.

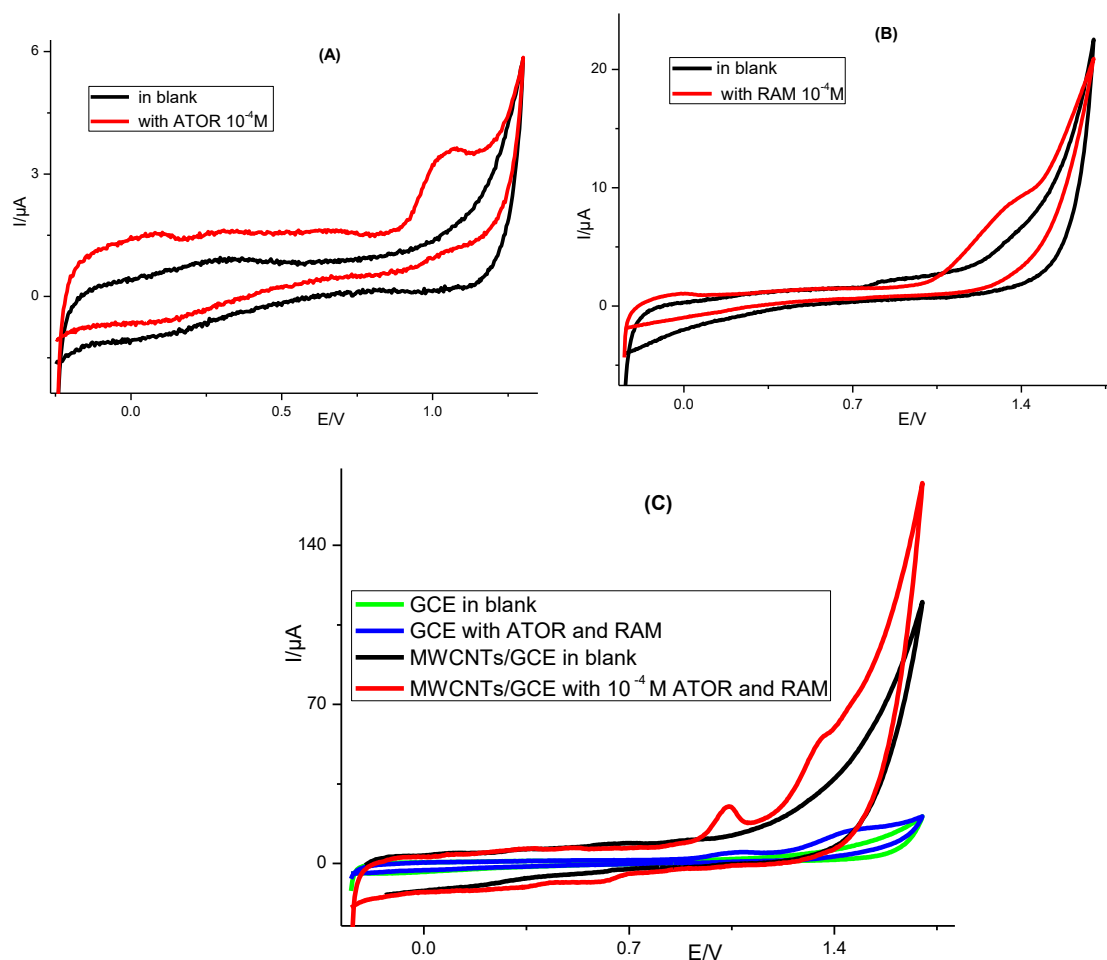


**Figure 8:** Cyclic voltammograms for (A) 0.1 mM ATOR and for (B) 0.1 mM RAM in 0.1 M H<sub>2</sub>SO<sub>4</sub> using a MWCNTs/GCE electrode. (C) CVs of 0.1 mM ATOR and RAM using the bare GCE and MWCNTs/GCE in 0.1 M H<sub>2</sub>SO<sub>4</sub> solution.

In addition, the SWV results shown in Fig. 9 for the bare GCE provided small current responses to ATOR and RAM. However, after modification of the GCE with the MWCNTs film, the oxidation peak current increased by a factor of 3 and 2.5 for ATOR and RAM, respectively. This indicates that MWCNTs/GCE has a good electro catalytic ability to the electrochemical reaction of ATOR and RAM. The peak-to-peak separation for ATOR and RAM was about 0.27 V. As a consequence, the simultaneous determination of ATOR and RAM is suitable at MWCNTs/GCE surface without any interference.

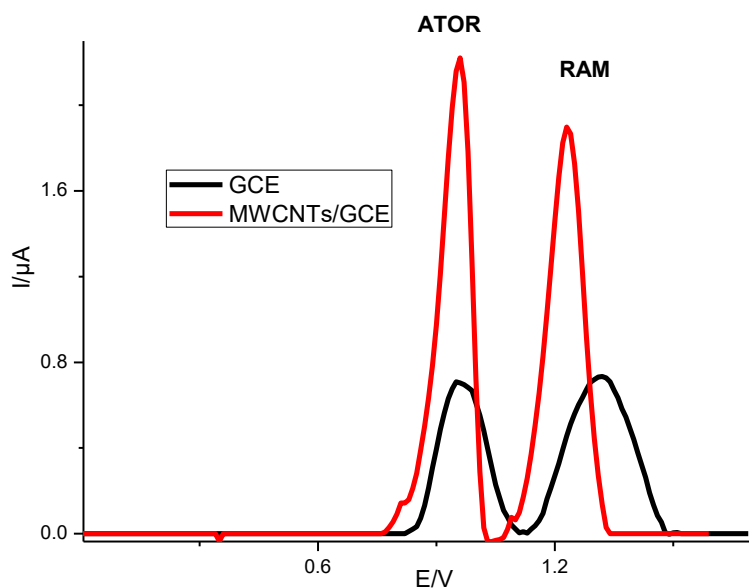


**Figure 9:** SWV of 0.1 mM ATOR and RAM using the bare GCE and MWCNTs/GCE in 0.1 M  $\text{H}_2\text{SO}_4$  solution.

### 3.3. Effect of MWCNT amounts:

Fig.10 shows the differential pulse voltammograms obtained with  $1 \times 10^{-4}$  M ATOR and RAM using the GCE with different amounts of MWCNT. It can be observed that an increase in the percentage of MWCNTs did not lead to an increase in the analytical response. In fact, amounts of MWCNTs in the glassy carbon higher than 2  $\mu\text{L}$  decreased the anodic response of ATOR and RAM. Therefore, the amount of MWCNTs chosen for the preparation of the sensor was 2  $\mu\text{L}$ .

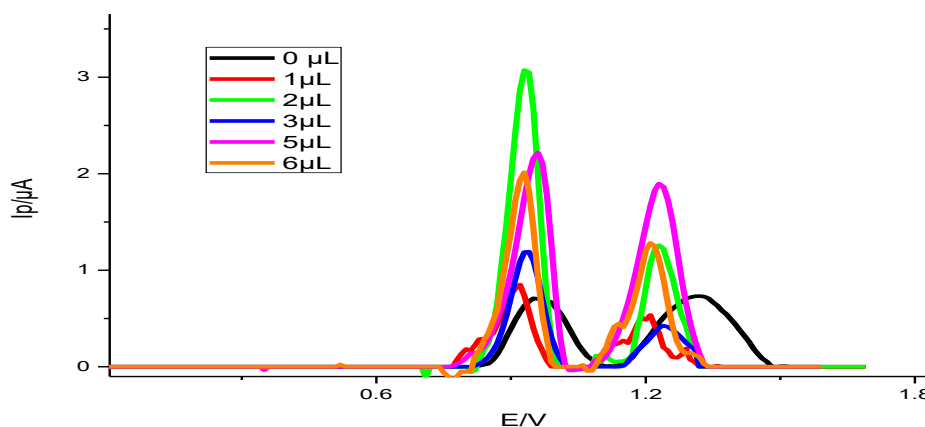


**Figure 10:** SW voltammograms obtained with  $1 \times 10^{-4}$  M ATOR and RAM in 0.1 M  $\text{H}_2\text{SO}_4$  (pH 1.0) using the MWCNTs/GCE sensor with different amounts of MWCNT.

### 3.4. Determination of electroactive surface area:

The electrochemically active surface area of the GCE and MWCNTs/GCE was examined with cyclic voltammetry based on Randles-Sevcik equation:

$$I_p = (2.69 \times 10^5) \times n^{3/2} A D_0^{1/2} C_0 \nu^{1/2}$$

where  $I_p$ ,  $n$ ,  $A$ ,  $C_0$ ,  $D_0$ , and  $\nu$  are the peak current, the number of electrons involved ( $n = 1$  in the  $[\text{Fe}(\text{CN})_6]^{3-/4-}$  redox system), the active surface area, the concentration of the reactant (5 mM), the diffusion coefficient of the  $[\text{Fe}(\text{CN})_6]^{3-/4-}$  ( $5.69 \times 10^{-6} \text{ cm}^2 \text{ s}^{-1}$ ) [32], and the scan rate, respectively. A pair of redox peaks was observed at GCE and MWCNTs/GCE. The peak current at modified electrode increases dramatically compared with that observed at bare GCE, suggesting that MWCNTs/GCE exhibits faster electron transfer kinetics and larger electroactive surface area compared with the bare GCE (Fig. 11). According to the above equation, the active surface area of GCE and MWCNTs/GCE was calculated as  $0.079 \text{ cm}^2$  and  $0.128 \text{ cm}^2$ , respectively. The results clearly show that the electrode modified with MWCNTs film had the larger active surface area, which result in higher sensitivity.

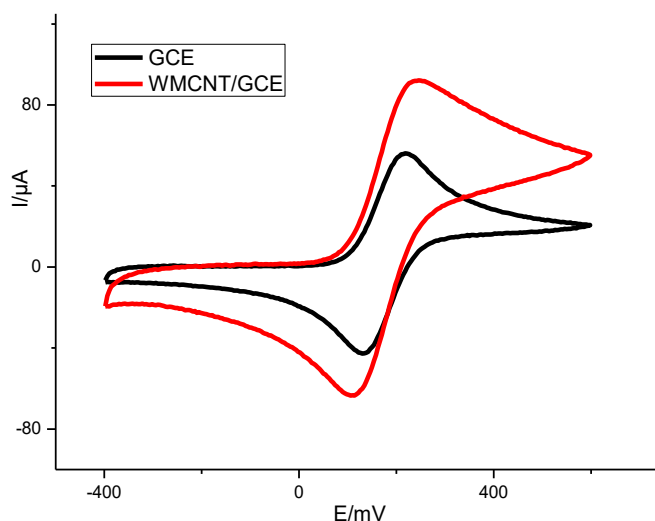


**Figure 11:** Cyclic voltammograms for GC electrode and MWCNTs/GC electrode in 5.0 mM  $K_3\text{Fe}(\text{CN})_6$  0.1 M KCl solution at scan rate of  $50 \text{ mV s}^{-1}$ .

### 3.5. The influence of pH:

The influence of pH on the oxidation process of 0.1 mM ATOR and RAM was investigated by SWVs in the pH range from 0.3 to 6 (Fig. 12A). As the pH increases, oxidation peak currents of both ATOR and RAM (Fig. 12B) increased until pH 3.0 and then decreased at higher pH values. Hence, pH 3.0 was selected as the optimum pH value for the simultaneous determination of both drugs. It is also observed that, following the pH from 0.3 to 6.0, the

peak potentials of ATOR (Fig. 13A) and RAM (Fig. 13B) shifted negatively, indicating the involvement of protons in the electrode reaction. The linear equation for ATOR was;

$$E_{pa} \text{ (V)} = -0.020\text{pH} + 0.824 \text{ (R}^2 = 0.96)$$

and for RAM;

$$E_{pa} \text{ (V)} = -0.042 \text{ pH} + 1.406 \text{ (R}^2 = 0.98)$$

The slopes of the respective equations were - 42 and - 20 mV/pH, implying that the equal number of electrons and protons participate in the RAM oxidation reaction and two-electrons and one-proton transfer to form ATOR cation.

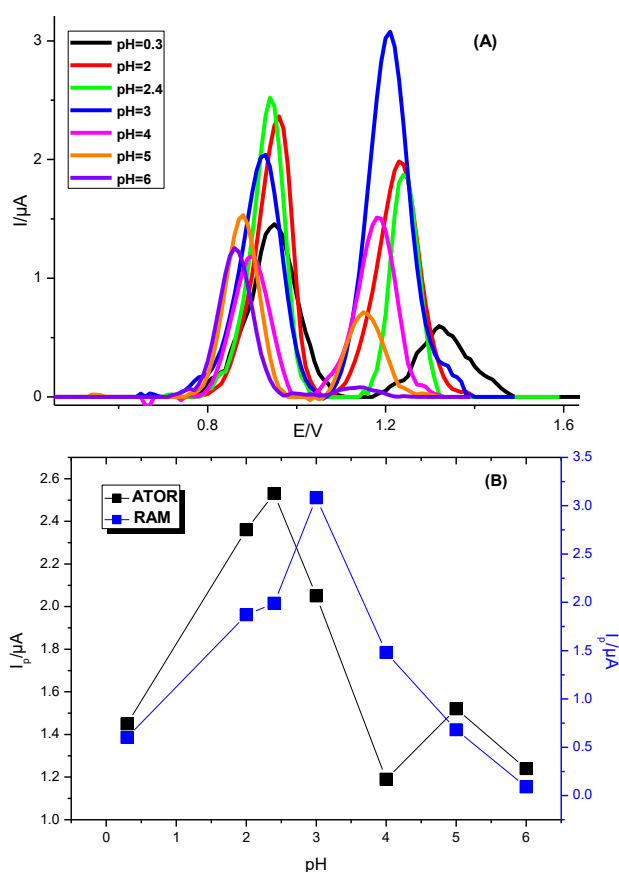


**Figure 12:** (A) SWV of 0.1 mM ATOR and RAM on MWCNTs/GCE at different pH value. (B) variation of  $I_p$  as function of pH value

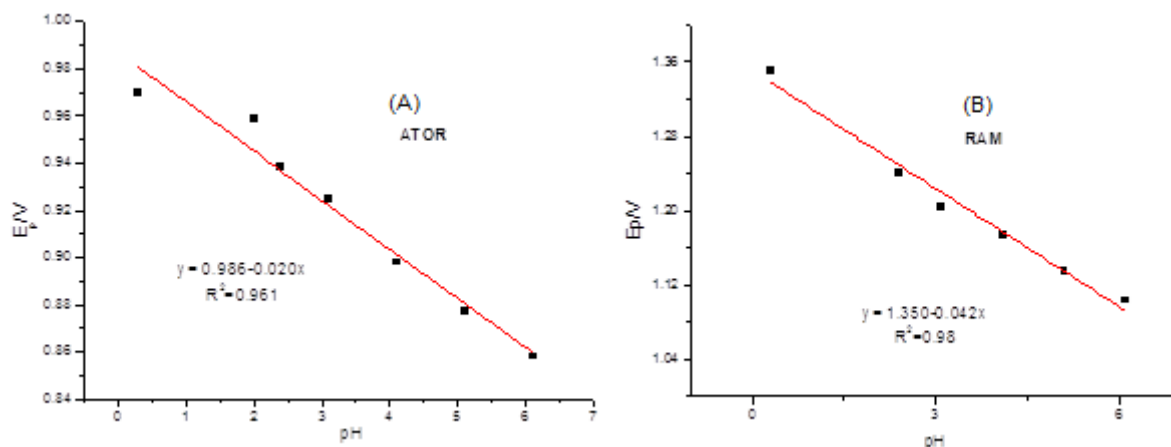


**Figure 13:** Variation of  $E_p$  as function of pH value (A) RAM and (B) ATOR.

### 3.6. The effect of scan rate:

The effect of scan rate on the peak currents of ATOR and RAM at the MWCNTs/GCE was characterized by cyclic voltammetry. As shown in Fig. 14, with increasing potential scan rate from 5 to 300  $\text{mV s}^{-1}$  a linear increase in the peak current for ATOR and RAM.

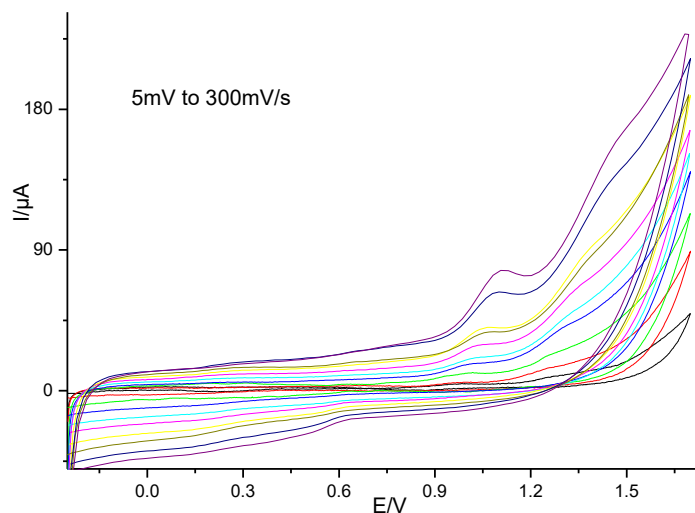


**Figure 14:** CVs of MWCNTs/GCE in 0.1 M BRB (pH 3.1) with 0.1 mM ATOR and RAM at different scan rates (5-300  $\text{mV s}^{-1}$ ).

The  $\log I_p$  vs.  $\log \nu$  plots for each process are presented in Fig. 15A, B. The linear relationships with slope values 0.72 for ATOR and 0.77 for RAM were obtained. These slope

values are between the theoretical values of 0.5, typical for diffusion-controlled process, and 1.0, reported for adsorption-controlled process [32].

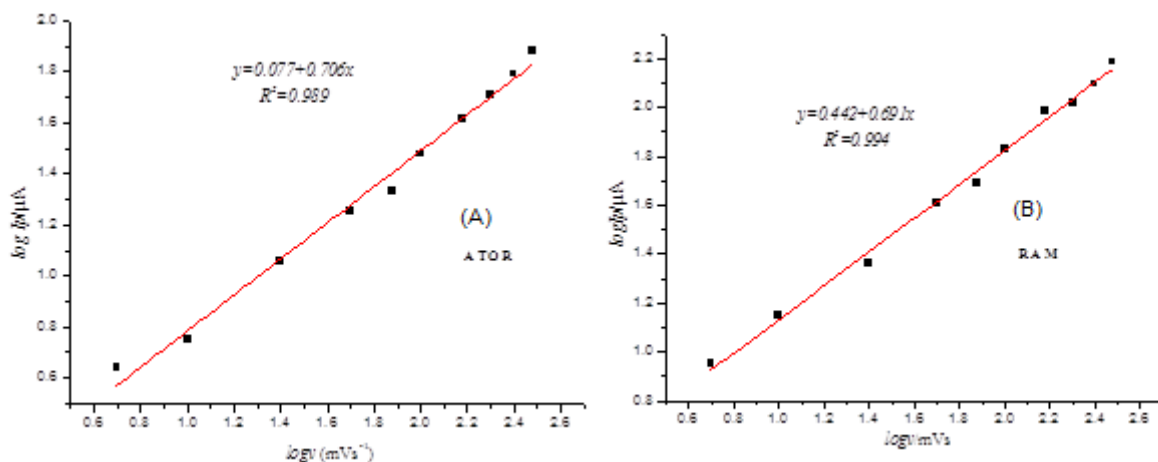


**Figure 15:** Logarithmic dependence of  $I_p$  on the logarithmic scan rate values (A) ATOR and (B) RAM.

So, to determine which of these processes dominated the electron transfer of both drugs, we constructed the plots of peak current versus potential scan rate (Fig. 16) and peak current versus square root of the scan rate (Fig. 17). As can be seen, an excellent linear dependence between the  $I_p$  and  $v$  with a correlation coefficient of 0.99 for ATOR and 0.98 for RAM were obtained, which suggested that the adsorption process was mostly dominated in electrochemical reaction of ATOR and RAM on MWCNTs/GCE.

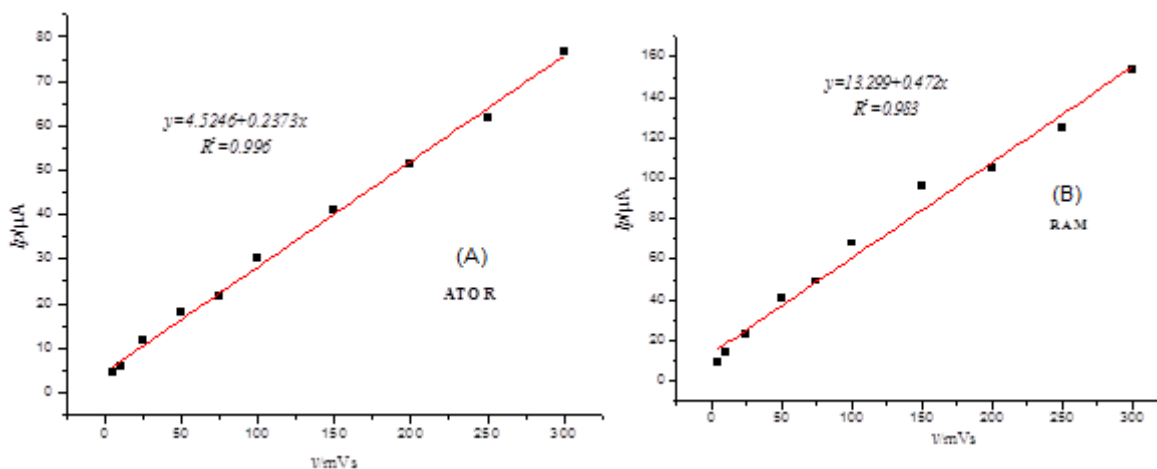


**Figure 16:** the plots of peak current ( $I_p$ ) versus potential scan rate ( $v$ ) (A) ATOR and (B) RAM.

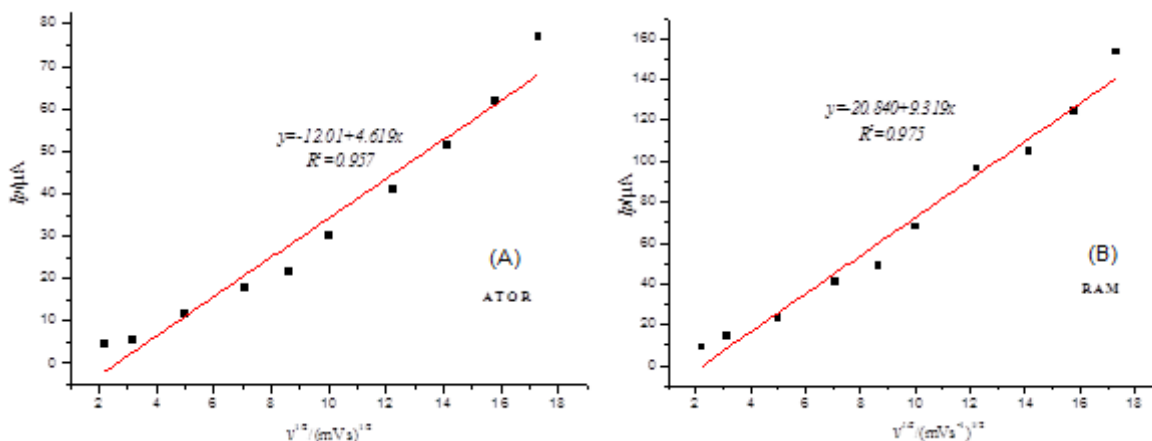


**Figure 17:** the plots of peak current ( $I_p$ ) versus square root of the scan rate ( $v^{1/2}$ ) (A) ATOR and (B) RAM.

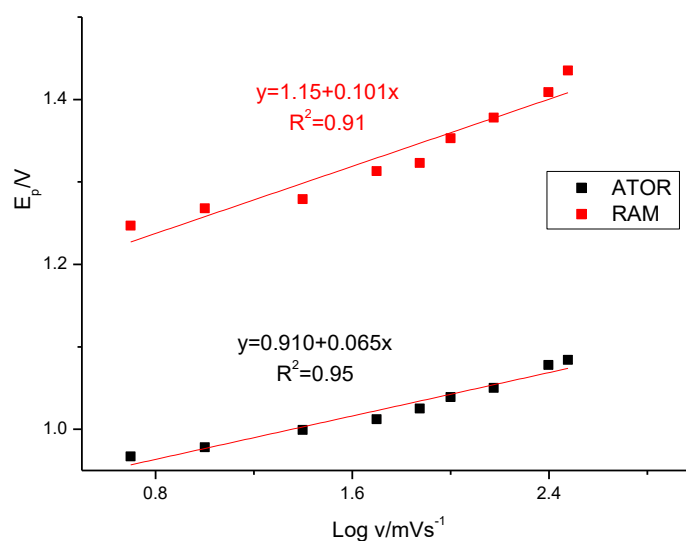


**Figure 18:** the plots of peak potential ( $E_p$ ) versus logarithmic scan rate values.

As well a linear dependence between the oxidation peak potential and the logarithm of scan rate were exposed as (Fig. 18):

$$E_p = 0.910 + 0.065 \log v \quad (R^2 = 0.95) \text{ for ATOR}$$

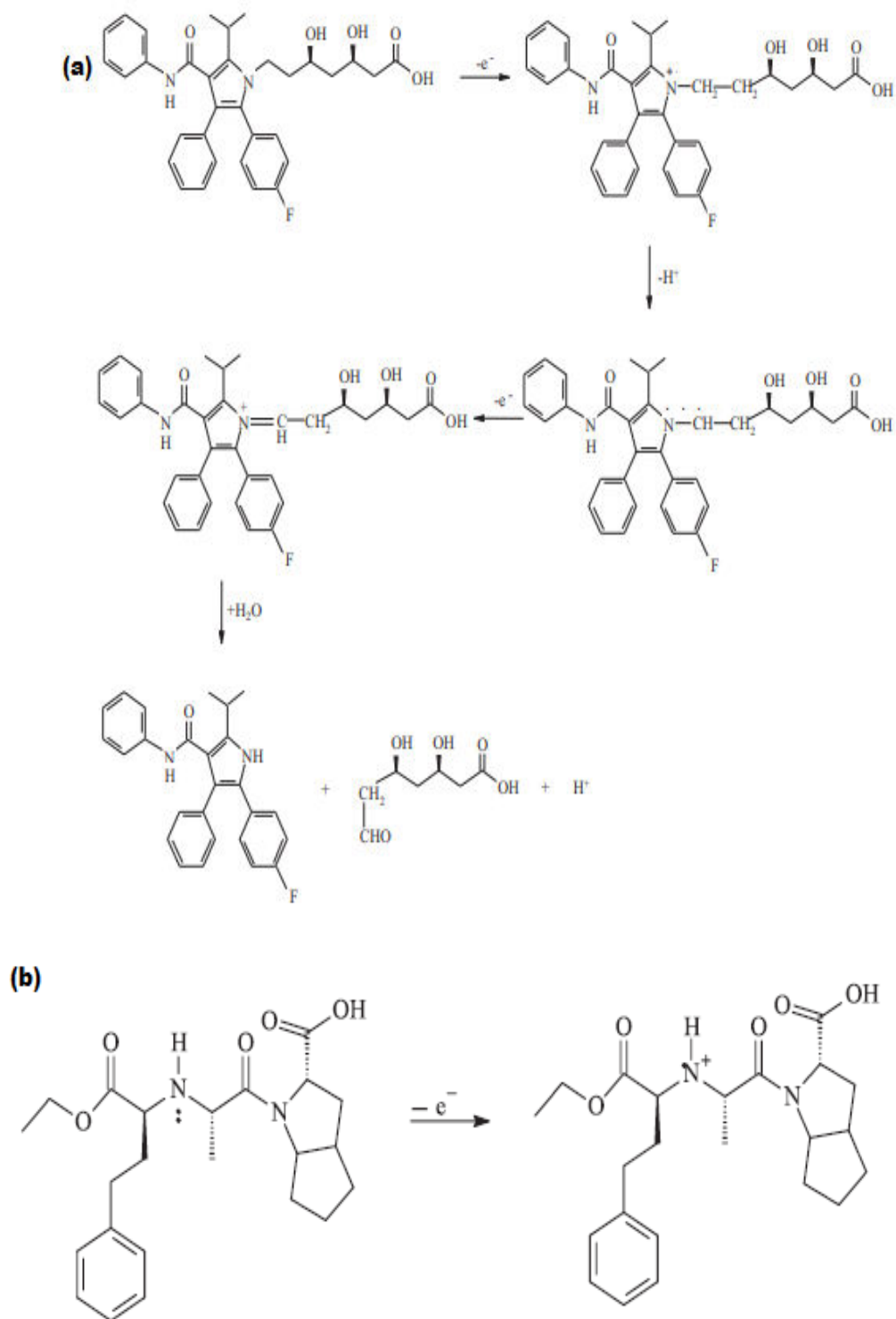
$$E_p = 1.150 + 0.101 \log v \quad (R^2 = 0.91) \text{ for RAM}$$

In case of irreversible electrode process, the electron transfer number in electrochemical reaction can be calculated using Laviron equation [33]:

$$E_{pa} = E^0 + 2.303RT/\alpha nF \log v$$

Where,  $E^{\circ}$  is formal potential,  $n$  is number of electrons transferred,  $\alpha$  is charge transfer coefficient, and. Other factors, such as  $F$  is Faraday's constant,  $T$  is absolute temperature, and  $R$  is ideal gas constant. Considering  $\alpha$  equal to 0.5 for irreversible reactions and based on the slope of equations 3 and 4, the number of electrons transferred in the oxidation of ATOR and RAM were calculated to be 1.81 ( $\approx 2$ ) and 1.17 ( $\approx 1$ ), respectively, which was consistent with previous studies [34, 35].

Considering this set of results and according to previously studies for both drugs, the electrode reaction of ATOR is probably to be oxidized to form pyridine cation, with contribution of two-electrons and one-proton. For RAM mechanism reaction, the RAM molecules involving the oxidation of the secondary amine group with the loss of one electron. The proposed mechanisms of the electrochemical reactions of both studied drugs may be proposed as following pathways in Scheme 1.



*Scheme 1: Proposed electro-oxidation mechanisms of ATOR (a) and RAM (b).*

### 3.7. Analytical Parameters:

The voltammetric determination of ATOR and RAM was carried out in BRB (pH 3.0) using SWV at the MWCNTs/GCE. The equal concentrations of ATOR and RAM changed synchronously from 10  $\mu\text{M}$  to 100  $\mu\text{M}$  and the obtained SWV responses were displayed in Fig. 19.

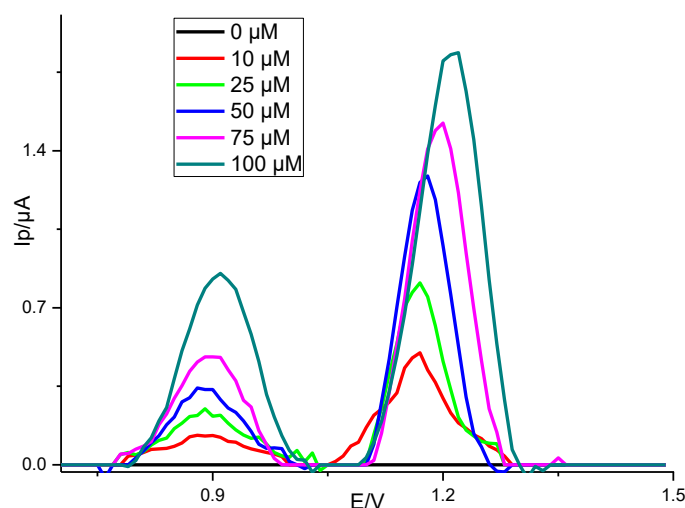


**Figure 19:** SWV responses for simultaneous addition of ATOR and RAM from 10 to 100  $\mu\text{M}$ .  
Experimental conditions: 0.1 M BRB (pH = 3.0) at MWCNTs/GCE.

The analytical curves obtained were linear for the concentration ranges from 10 to 100  $\mu\text{M}$  for ATOR and RAM (Fig. 20). The equations associated to these analytical curves were:

$$I_p(\mu\text{A}) = 0.010 + 0.007 C_{\text{ATOR}}(\mu\text{M}) \quad (R^2 = 0.98) \text{ for ATOR}$$

and

$$I_p(\mu\text{A}) = 0.38 + 0.016 C_{\text{RAM}}(\mu\text{M}) \quad (R^2 = 0.98) \text{ for RAM}$$

Both LOD and LQD values were calculated using the relations

$$\text{LOD or LOQ} = ks/m$$

where  $s$  is the standard deviation of the 3 repeated peak currents of the lowest concentration of the range,  $m$  is the slope of the linearity curve,  $k = 3$  for LOD and 10 for LOQ [36]. The necessary validation steps and calculated analytical parameters for both drugs such as LOD, LOQ, precision, sensitivity, etc. listed as details in Table 1.

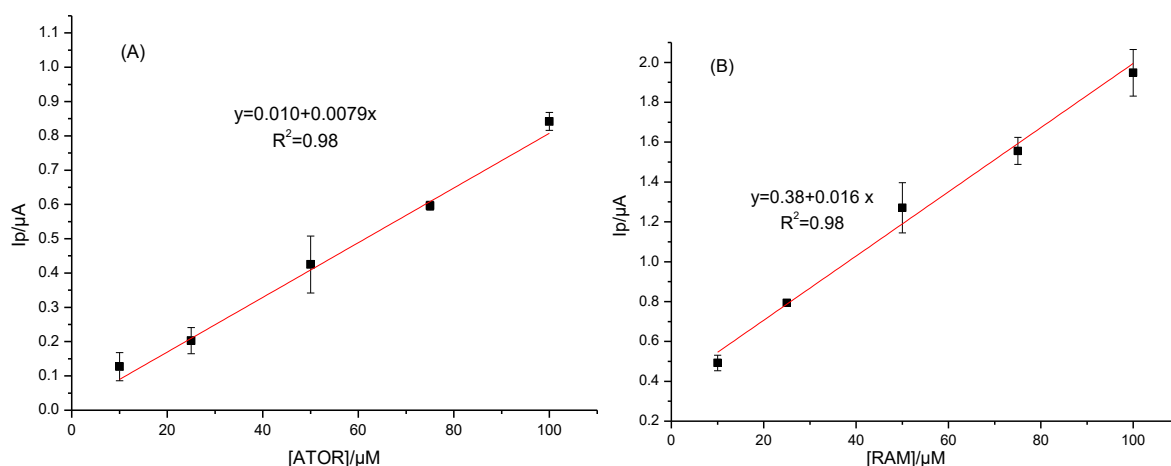


**Figure 20:** The calibration curves for peak current vs. concentration for (A) ATOR and (B) RAM.

**Table 1:** Regression data of the calibration curve for quantitative determination of ATOR and RAM by SWV method in bulk solution.

	0.1 M BRB (pH 3.1)	
	ATOR	RAM
Peak potential (V)	0.87	1.13
Linearity range ( $\mu\text{M}$ )	10-100	10-100
Slope ( $\mu\text{A } \mu\text{M}^{-1}$ )	0.007	0.016
SE of slope	$4.8 \times 10^{-4}$	$9.4 \times 10^{-4}$
Intercept ( $\mu\text{A}$ )	0.01	0.38
SE of intercept	0.03	0.02
Correlation coefficient ( $R^2$ )	0.98	0.98
LOD ( $\mu\text{M}$ )	2.57	1.87
LOQ ( $\mu\text{M}$ )	8.57	6.25
Within-day of the peak current (RSD%) <sup>a</sup>	4.68	1.46
Within-day of the peak potential (RSD%) <sup>a</sup>	0.85	0.60

<sup>a</sup> Obtained from average of three experiments.

Table 2 shows a comparison between analytical results of the proposed method and some other methods involved in the simultaneous determination of ATOR and RAM. The analytical performance of the present method is quite comparable with the published analytical method. Moreover, the proposed method did not require any sample pretreatments or time-consuming extractions steps. Once again, it should be mentioned that there is no relating report on

electrochemical methods for the simultaneous determination of ATOR and RAM until this work was undertaken.

**Table 2.** Comparison of the analytical parameters obtained using different techniques for the determination of ATOR and RAM.

Technique	Concentration range ( $\mu\text{M}$ )		LOD ( $\mu\text{M}$ )		Ref.
	ATOR	RAM	ATOR	RAM	
HPLC	8.95-44.75	12.0-60.0	0.78	0.68	[37]
RP-HPLC	3.58-35.8	12.0-120	$1.6 \times 10^{-5}$	$1.03 \times 10^{-4}$	[38]
HPLC	7.16-57.2	9.60-52.81	0.49	0.86	[39]
UV Spectrophotometric	3.58-17.90	2.40-12.0	0.823	0.672	[40]
Electrochemical method	10-100	10-100	2.57	1.87	This work

#### **4. Conclusion and perspectives:**

In this work, a fast and sensitive electrochemical sensor (GCE/MWCNTs) for the simultaneous determination of binary a mixture of Atorvastatin and Ramipril is elaborated. The MWCNTs film provides a high specific surface area and improves the conductivity of the modified electrode. The behavior of both drugs at MWCNTs indicates that this electrode might be used for analytical purposes, particularly as a sensor. Electro-analytical measurements were applied with the square wave voltammetry (SWV), the technique was developed for the simultaneous electrochemical determination of ATOR and RAM. This technique could provide a favorable perspective in the fabrication of electrochemical platforms based on electrodes modified with MWCNTs film for simultaneous detection at least two drugs. In comparison to published methods, the proposed sensor is speedy and inexpensive for drugs sensing without any time-consuming sample extraction, evaporation or filtration steps. Consequently, this method has the potential for being an attractive alternative for the simultaneous determination of ATOR and RAM in pharmaceutical and biological samples.

In perspectives, the study carried out with this sensor, the first results which are promising, remains to be finalized.

First, the interference study, surface renewal and response stability of the modified electrode must be evaluated based on analytical parameters to provide a reliability of this developed sensor.

Then, the detection field must be extended to determine of ATOR and RAM in pharmaceutical and biological samples. This will make it possible to better appreciate the functionalization MWCNTs developed, in order to provide a favorable perspective in the fabrication of electrochemical platforms for simultaneous detection of these two drugs.

## REFERENCES:

- [1] E. A. Taha, A. K. A., M. M. Fouad, and Z. M. Yousef, *Anal. Bioanal. Electrochem*, 11 (2019) 150
- [2] R. W. Piepho, , *Am. J. Health-Syst. Pharm* (2000), pp. 57.
- [3] Arnold, J. M. O, Yusuf, S.Young, J. Mathew, J. Johnstone, D. Avezum, A. Lonn, E. Pogue, J. Bosch, *J. Circulation* 107 (2003) 1284.
- [4] Chawla A Pooja, P. S., Monika. 9 (2019) 88.
- [5] Yogesh B. Zambare, S. R. K., C.C. Simpi, *Journal of Pharmacy Research Vol.2.Issue.* (27-02-2009),
- [6] Manisha B. Jadhav, S. S. S., Sachin R. Tajane, K.N.Tarkase, I. J. Pharma. . *Pharm. Sci* 4 (2012) 387.
- [7] Boyka G Tsvetkova, P. L. *J Chem Pharm Res.* 5 (2013) 168
- [8] S. Li , K. Peng , Z. Ma , X. Zhang , S. Fu, X. Li, Linlin; Li, A. H. a. J. J, *Molecules* 17 (2012) 2663.
- [9] Ramakrishna, C. V. a. K., *Rasayan journal chemistry* 8 (2015) 404.
- [10] C. Ashish, B. M. a. P. C, *Analytical & Bioanalytical Techniques* \*(2015)\*\*.
- [11] Chapter, I. Electrochemical methods. *Current Separations* (2002), 51-53.
- [12] Ciucu, A. A., *Journal of Biosensors & Bioelectronics* (2014), 5, 1.
- [13] Batchelor-McAuley, C. Dickinson, E. J. Rees, N. V. Toghil, K. E. Compton, R. G.. *Analytical chemistry* 84 (2012) 669.
- [14] R.W. Murray, E. A. Firt, R.A. Durst, *Anal Chem* 59 (1987) 379A.
- [15] R.A. Durst, A.J. Baumner, R.W. Murray, R.P. Buck, C.P. Andrieux, *Pure & Appl. Chem.*,69 (1997) 1317
- [16] Rodes, A. Feliu, J. Aldaz, A. Clavilier, J. *Journal of electroanalytical chemistry and interfacial electrochemistry*, 271 (1989) 127.
- [17] Uosaki, K. Sato, Y. Kita, H., *Langmuir* 7 (1991) 1510.
- [18] Huang, T. Lu, R.; Su, C. Wang, H. Guo, Z. Liu, P. Huang, Z. Chen, H. Li, T., *ACS applied materials & interfaces* , 4, (2012), 2699-2708.
- [19] Bruti, E. M. Giannetto, M. Mori, G. Seeber, R.. *Electroanalysis: An International Journal Devoted to Fundamental and Practical Aspects of Electroanalysis* ,11, (1999), 565-572.

- [20] Sajid, M. Nazal, M. K. Mansha, M. Alsharaa, A. Jillani, S. M. S. Basheer, C., *TrAC Trends in Analytical Chemistry*, 76 (2016) 15.
- [21] R.W. Murray, *Journal of Chemical Education* 4 (1983) 302.
- [22] H. R. Zare, N. Nasirizadeh, F. Chatraei, S. Makarem, *Electrochim. Acta* 54 (2009) 2828.
- [23] J. Wang, M. Musameh, *Analyst* 11 (2003) 1382.
- [24] M. Musameh, J. Wang, A. Merkoci, Y. Lin, *Electrochem. Commun.* 4 (2002) 743.
- [25] Z. Wang, Q. Liang, Y. Wang, G. Luo, *J. Electroanal. Chem.* 540 (2003) 129
- [26] H. Luo, Z. Shi, N. Li, Z. Gu, Q. Zhuang, *Anal. Chem.* 73 (2001) 915.
- [27] J. Wang, M. Mosameh, Y. Lin, *J. Am. Chem. Soc.* 125 (2003) 2408.
- [28] G. Selvarani, S.K. Prashant, A.K. Sahu, P. Sridhar, S. Pitchumani, A.K. Shukla, *J. Power Sources* 178 (2008) 86.
- [29] A.J. Bard, L.R. Faulkner, *Electrochemical Methods: Fundamentals and Applications*, 2nd Ed., John Wiley & Sons, Hoboken NJ (2001)
- [30] D. A. Skoog, D. M. West, and F. J. Holler, *Fundamentals of Analytical chemistry*, 7th Edition, Harcourt, (1996).
- [31] F. Scholz (Ed), *Electro analytical Methods Guide to Experiments and applications* springer, (2005).
- [32] A. J. Bard , L. R. Faulkner, in *Electrochemical methods: Fundamentals and Applications* ,Wiley, New York, (1980).
- [33] E. Laviron, *J. Electroanal. Chem. Interfacial Electrochem.* 100, (1979), 263-270.
- [34] Eskiköy, D.Durmuş,Z.Kiliç,E,*Collection of Czechoslovak Chemical Communications*, 76, (2012), 1633-1649.
- [35] M. Douliche, M. Bakirhan, N. K. Saidat, B.Ozkan, S.A., *Journal of The Electrochemical Society* ,167(2020) 027511.
- [36] Şengül, Ü. , *Journal of food and drug analysis* 24(2016) 56.
- [37] S.M. Patole, L.V. Potale, L. Khodke, A. Damle, M. , *Int J Pharm Sci Rev Res* 4 (2010) 40.
- [38] R. Sharma, S. Khanna, P. M.Ganesh *Journal of Chemistry* 9 ( 2011) 2177.
- [39] N. Gowda, R. Tekal, R. Thangavelu, *Journal of food and Drug analysis*, 20 (2012) 577.
- [40] A. Sankar, T. Vetrichelvan, D. Venkappaya, *Acta Pharmaceutica* 61(2011)283.